CSIRO PUBLISHING

Australian Journal of Physics

Volume 51, 1998

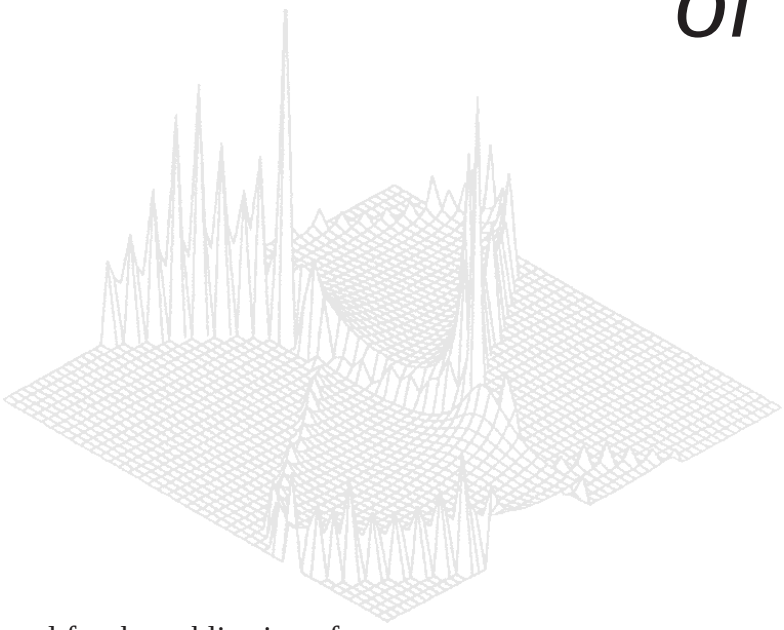

A journal for the publication of
original research in all branches of physics

www.publish.csiro.au/journals/ajp

All enquiries and manuscripts should be directed to
Australian Journal of Physics
CSIRO PUBLISHING
PO Box 1139 (150 Oxford St)
Collingwood Telephone: 61 3 9662 7626
Vic. 3066 Facsimile: 61 3 9662 7611
Australia Email: peter.robertson@publish.csiro.au

Published by **CSIRO** PUBLISHING
for CSIRO and the
Australian Academy of Science

Aust. J. Phys., 1998, **51**, 943–57

Elastic Properties of Cs_2HgBr_4 and Cs_2CdBr_4 Crystals

A. V. Kityk, A. V. Zadorozhna, Ya. I. Shchur, I. Yu. Martynyuk-Lototska, Ya. Burak and O. G. Vlokh

Institute of Physical Optics, Dragomanova str 23,
290005 Lvov, Ukraine.

Abstract

Using ultrasonic velocity measurements, all components of the elastic constant matrix C_{ij}, elastic compliances matrix S_{ij}, and linear compressibility constants matrix K_{ij} of orthorhombic Cs_2HgBr_4 and Cs_2CdBr_4 crystals have been determined over a wide temperature range, including the region of the phase transition from the normal to the incommensurate phase. Results obtained are considered within the framework of the phenomenological theory. Preliminary analysis of the acoustical properties at room temperature clearly indicates that both crystals are relatively important materials for acousto-optical applications.

1. Introduction

Caesium mercury tetrabromide (Cs_2HgBr_4) and caesium cadmium tetrabromide (Cs_2CdBr_4) are members of the large family of β-K_2SO_4 structure materials. Many of these materials show an incommensurate phase in their sequence of structural phase transformations. In general, the incommensurate phase is terminated by a lock-in transition, and the resulting commensurate superstructure phase is an improper ferroelectric or ferroelastic. The two materials considered in the present paper, Cs_2HgBr_4 and Cs_2CdBr_4, are unusual among the A_2BX_4 crystals, since the lock-in transition occurs at the centre of the Brillouin zone ($\boldsymbol{k}_C = 0$) rather than at $\boldsymbol{k}_C = ma^*/n$ ($a^* = 2\pi/a$ is the reciprocal lattice parameter), which usually takes place in the incommensurate dielectrics. Thus the incommensurate phases of these crystals belong to type II according to the classification of Bruce and Cowley (1978). At atmospheric pressure these crystals have the following phase sequences (Plesko *et al.* 1980*a*, 1981; Maeda *et al.* 1983):

Cs_2HgBr_4:

$$\text{phase I} \xrightarrow{T_1=243K} \text{phase II} \xrightarrow{T_C=230K}$$

$$\text{phase III} \xrightarrow{T_1=165K} \text{phase IV} \xrightarrow{T_2=85K} \text{phase V}.$$

 10.1071/PH98037 0004-9506/98/060943$05.00

Cs_2CdBr_4:

$$\text{phase I} \xrightarrow{T_1=252K} \text{phase II} \xrightarrow{T_C=237K} \text{phase III} \xrightarrow{T_1=158K} \text{phase IV}.$$

Both crystals undergo three analogous consecutive phase transitions: from the orthorhombic normal phase I (space group *Pnma*) to the incommensurate phase II at $T = T_I$, to the monoclinic proper ferroelastic phase III (space group $P2_1/n11$) at $T = T_C$ and to the triclinic proper ferroelastic phase IV (space group $P\bar{1}$) at $T = T_1$. In addition, Cs_2HgBr_4 also exhibits a low-temperature structural phase transition into the triclinic phase V (space group $P\bar{1}$) with a doubled period of the unit cell in the *b*-direction at $T = T_2$ (Plesko *et al.* 1980*a*, 1981). The soft mode associated with the normal–incommensurate phase transition in these crystals consists mainly of the rotation of the rigid XBr_4 tetrahedra (X = Cd, Hg) around the *a*-axis (Plesko *et al.* 1980*b*; Nakatama *et al.* 1987). Plesko *et al.* (1980*a*, 1980*b*) reported NQR and X-ray results indicating that both of these crystals undergo transitions at T_I from the normal to the incommensurate phase, modulated in the *X*-direction with $\boldsymbol{k}_0 \approx 0{\cdot}15a^*$, and then at the lock-in transition, T_C, to the monoclinic $P2_1/n11$ phase which restores the unit cell to its initial size.

Acoustic and optical measurements were used in the investigation of the pressure–temperature (P–T) phase diagram of Cs_2HgBr_4 and Cs_2CdBr_4 crystals (Kityk *et al.* 1993). It was shown that the incommensurate phase in the P–T phase diagram disappears in the triple point (P_K, T_K), where the two boundaries of the incommensurate phase merge into one line of the ferroelastic phase transition. The nature of the corresponding triple point in the P–T phase diagram of crystals has been considered in detail only within the framework of the phenomenological theory (Kityk *et al.* 1993; Vlokh *et al.* 1989), whereas the microscopic aspects of this phenomenon remain unknown.

The microscopic model of the lattice instability of Cs_2HgBr_4 and Cs_2CdBr_4 induced by high hydrostatic pressure will be considered in our further work. In general, for ionic crystals it is frequently based on the computer simulation of the lattice dynamics within the rigid-ion model in the harmonic approximation. Recently, such a model was successfully applied in the microscopic consideration of the high-pressure-induced proper ferroelastic instability in the isostructural compound Cs_2HgCl_4 (Kityk *et al.* 1998). The influence of anharmonicity, which causes the lattice instability at the structural phase transition, has been introduced into this simulation indirectly through the changes of the lattice parameters under applied hydrostatic pressure. The coefficients of the lattice compressibility, which are necessary in this case, have been determined from the total elastic constant matrix. Unfortunately, previous acoustical measurements (Kityk *et al.* 1993) for Cs_2HgBr_4 and Cs_2CdBr_4 were not completed. They concerned only some diagonal components of the elastic constant matrix. Thus the total picture of the elastic behaviour around the incommensurate phase transition has not been ascertained. This problem is solved for the first time in the present work, where we consider the behaviour of all elastic moduli C_{ij}, elastic compliances S_{ij}, and linear compressibility constants K_{ij} in a wide temperature range including the region of the incommensurate phase transition at $T = T_I$. The results obtained are analysed within the framework of the phenomenological theory.

Finally, we must note that complete information about the elastic properties of the Cs_2HgBr_4 and Cs_2CdBr_4 crystals is also very important from the point of view of their application in acousto-optics. In particular, previous acoustical investigations indicate that these crystals probably would be potentially useful for acousto-optical applications, on account of their relatively low values of the velocities of the longitudinal and transverse ultrasonic waves.

2. Experimental

Single crystals of Cs_2HgBr_4 and Cs_2CdBr_4 were grown from the melt by the Bridgman method. The crystallographic axes were determined by the X-ray diffraction method. We used the following crystallographic orientation: $c > a > b$ ($c \sim \sqrt{3}b$, where a is the pseudohexagonal axis). The plane parallel specimens are typically of $4{\times}4{\times}4\ \mathrm{mm}^3$ size.

Velocity changes of the longitudinal and transverse ultrasonic waves were measured by the pulse-echo overlap method (Papadakis 1967) with an accuracy of the order of 10^{-4}–10^{-5}. The accuracy of the absolute velocity determination was about $0{\cdot}5\%$. The acoustic waves in the samples were excited by $LiNbO_3$ transducers (resonance frequency $f = 10\ \mathrm{MHz}$, bandwidth $\Delta f = 0{\cdot}1\ \mathrm{MHz}$ and acoustic power, $P_\mathrm{a} = 1$–$2\ \mathrm{W}$). The acoustic investigations were performed with a rate of temperature change of about $0{\cdot}3\ \mathrm{K\ min}^{-1}$.

3. Experimental Results and Discussion

The elastic constants are usually referred to an orthonormal set of axes $X = 1$, $Y = 2$, $Z = 3$, which, in the case of the orthorhombic structure, possess a standard orientation in respect to the orthonormal principal crystallographic axes, $a \equiv X$, $b \equiv Y$, $c \equiv Z$. Here we report a complete determination of the elastic constant matrix $C_{klmn} \equiv C_{ij}$ (where $i,j = 1$–6, $1 \equiv 11$, $2 \equiv 22$, $3 \equiv 33$, $4 \equiv 23$, $5 \equiv 13$, $6 \equiv 12$), via measurements of the ultrasonic phase velocities along different crystallographic directions. There are nine independent nonzero elastic constants C_{11}, C_{22}, C_{33}, C_{44}, C_{55}, C_{66}, C_{12}, C_{13}, C_{23} for orthorhombic symmetry. Direct and simple relations between measured velocities and elastic constants are possible only for the diagonal elements (C_{ii}) of the elastic constant matrix. All other constants occur coupled together in more complicated relationships. The determination of all nine elastic constants of the orthorhombic system is therefore demanding, both experimentally and computationally. To determine all nine elastic constants, measurements of the velocities of the longitudinal and transverse ultrasonic waves were required in at least six different directions: [100], [010], [001], [110], [101], [011]. Table 1 gives the details of the nine ultrasonic waves that have been used in our studies. The relationships between measured velocities, V_i, and the elastic constants, C_{ij}, follow from the Christoffel equation (see, for example, Prawer *et al.* 1985):

$$|\lambda_{lm} - \rho V^2 \delta_{lm}| = 0, \quad l, m = 1 - 3\,,$$

$$\lambda_{lm} \equiv \lambda_j = Q_{ji} L_i, \quad i, j = 1 - 6\,, \tag{1}$$

$$Q_{ji} = \begin{bmatrix} C_{11} & C_{66} & C_{55} & 0 & 0 & 0 \\ C_{66} & C_{22} & C_{44} & 0 & 0 & 0 \\ C_{55} & C_{44} & C_{33} & 0 & 0 & 0 \\ 0 & 0 & 0 & (C_{23}+C_{44})/2 & 0 & 0 \\ 0 & 0 & 0 & 0 & (C_{13}+C_{55})/2 & 0 \\ 0 & 0 & 0 & 0 & 0 & (C_{12}+C_{66})/2 \end{bmatrix}, \quad L_i = \begin{bmatrix} l^2 \\ m^2 \\ n^2 \\ 2mn \\ 2ln \\ 2lm \end{bmatrix},$$

where l, m, n are the direction cosines of the propagation vector $\boldsymbol{q}$, and ρ is the crystal density. Using equation (1) for the experimental geometries presented in Table 1, we obtained the following relations between ultrasonic wave velocities V_i and elastic constants C_{ij}:

$$C_{11} = \rho V_1^2, \qquad C_{22} = \rho V_2^2, \qquad C_{33} = \rho V_3^2\,,$$

$$C_{44} = \rho V_4^2, \qquad C_{55} = \rho V_5^2, \qquad C_{66} = \rho V_6^2\,,$$

$$C_{12} = \pm 0{\cdot}5[(4\rho V_9^2 - C_{11} - C_{22} - 2C_{66})^2 - (C_{11} - C_{22})^2]^{1/2} - C_{66}\,, \tag{2}$$

$$C_{13} = \pm 0{\cdot}5[(4\rho V_8^2 - C_{11} - C_{33} - 2C_{55})^2 - (C_{11} - C_{33})^2]^{1/2} - C_{55}\,,$$

$$C_{23} = \pm 0{\cdot}5[(4\rho V_7^2 - C_{33} - C_{22} - 2C_{44})^2 - (C_{22} - C_{33})^2]^{1/2} - C_{44}\,.$$

Table 1. Ultrasonic wave velocities in Cs_2HgBr_4 and Cs_2CdBr_4 crystals
PT = pure transverse, PL = pure longitudinal, QL = quasilongitudinal

V_i	Direction of wave propagation $\boldsymbol{q}$	Approximate wave displacement direction $\boldsymbol{e}$	Velocity at 293 K (m s^{-1}) Cs_2HgBr_4	Cs_2CdBr_4	Type
V_1	[100]	[100]	2171·9	2292·9	PL
V_2	[010]	[010]	1781·3	1895·7	PL
V_3	[001]	[001]	1758·0	1916·7	PL
V_4	[010]	[001]	804·9	843·0	PT
V_5	[100]	[001]	916·2	1016·6	PT
V_6	[100]	[010]	811·3	885·0	PT
V_7	[011]	[011]	1726·3	1831·4	QL
V_8	[101]	[101]	1905·8	2048·3	QL
V_9	[110]	[110]	1866·9	1994·1	QL

The measured temperature dependences of the velocities for the pure longitudinal: $V_1(\boldsymbol{q}||\boldsymbol{a}, \boldsymbol{e}||\boldsymbol{a})$, $V_2(\boldsymbol{q}||\boldsymbol{b}, \boldsymbol{e}||\boldsymbol{b})$ and $V_3(\boldsymbol{q}||\boldsymbol{c}, \boldsymbol{e}||\boldsymbol{c})$; pure transverse: $V_4(\boldsymbol{q}||\boldsymbol{b}, \boldsymbol{e}||\boldsymbol{c})$, $V_5(\boldsymbol{q}||\boldsymbol{a}, \boldsymbol{e}||\boldsymbol{c})$ and $V_6(\boldsymbol{q}||\boldsymbol{a}, \boldsymbol{e}||\boldsymbol{b})$; and quasilongitudinal: $V_7(\boldsymbol{q}||[011]$, $\boldsymbol{e}||[011])$, $V_8(\boldsymbol{q}||[101], \boldsymbol{e}||[101])$ and $V_9(\boldsymbol{q}||[110], \boldsymbol{e}||[110])$ acoustic modes of Cs_2HgBr_4 and Cs_2CdBr_4 are shown in Figs 1*a* and 1*b*, respectively. Clear kinks in the temperature dependences of the ultrasonic velocities (V_1, V_2, V_3, V_7, V_9) occur for both Cs_2HgBr_4 and Cs_2CdBr_4 in the region of the second-order phase

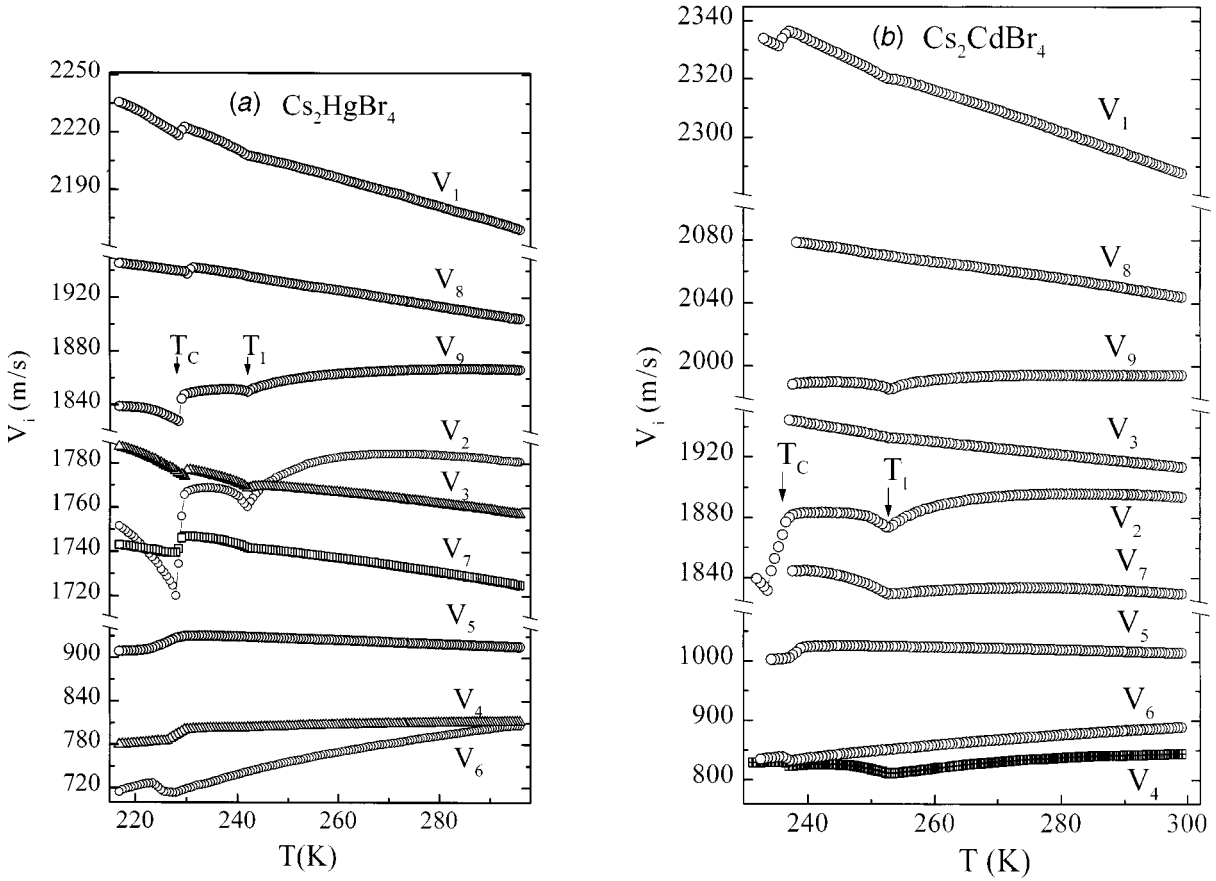

Fig. 1. Temperature dependences of the ultrasonic wave velocities of (a) Cs_2HgBr_4 and (b) Cs_2CdBr_4 crystals.

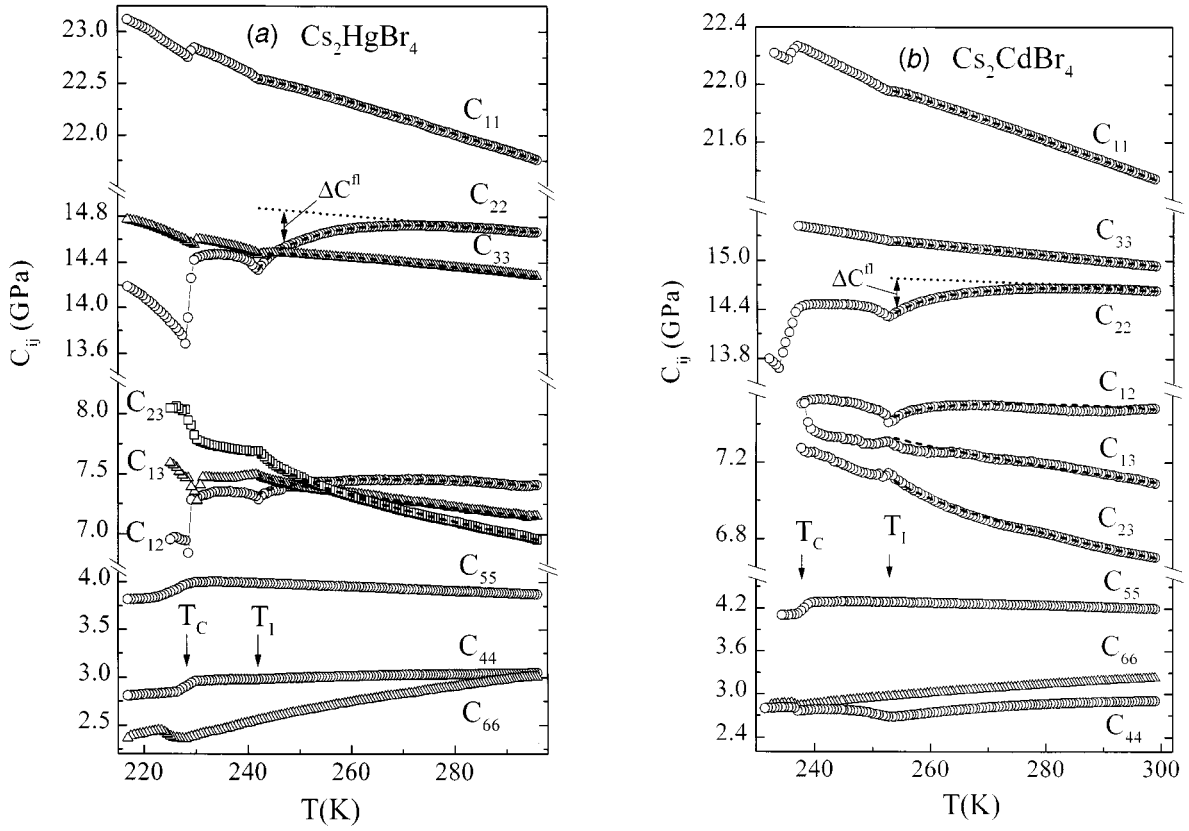

Fig. 2. Temperature dependences of the elastic constants C_{ij} of (a) Cs_2HgBr_4 and (b) Cs_2CdBr_4 crystals.

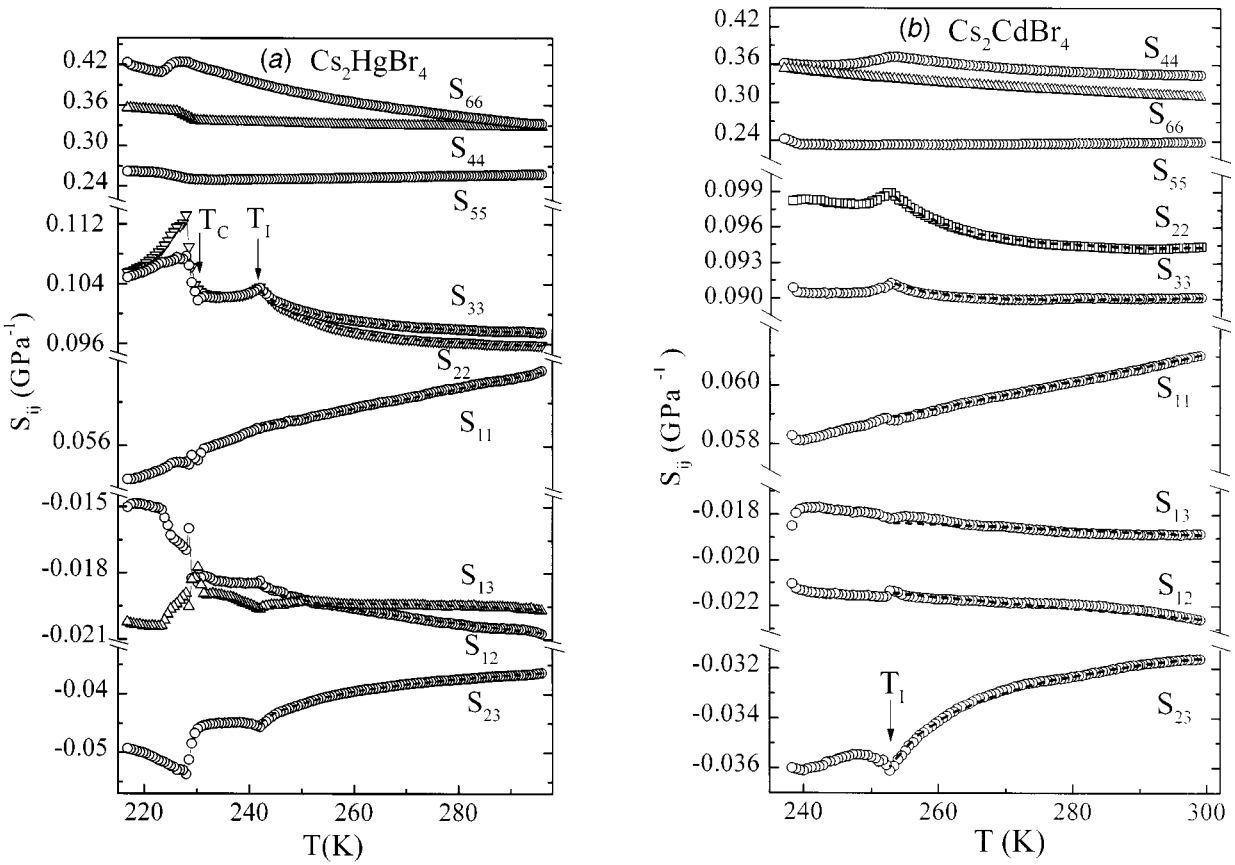

Fig. 3. Temperature dependences of the elastic compliances S_{ij} of (a) Cs_2HgBr_4 and (b) Cs_2CdBr_4 crystals.

transition from the normal to the incommensurate phase at $T = T_{\mathrm{I}}$, whereas in the vicinity of the first-order phase transition at $T = T_{\mathrm{C}}$ considerable jump-like changes are observed. A strong ultrasonic attenuation complicates the acoustic investigation near T_{C} for the V_3, V_7, V_8 and V_9 modes of Cs_2CdBr_4, so they are presented only above T_{C}.

Fig. 2 shows the temperature dependences of all nine elastic constants C_{ij} for both compounds that have been determined from the data presented in Fig. 1 using equations (2). For the components C_{12}, C_{13} and C_{23} we obtained two solutions depending on whether the positive or negative square roots were taken in (2). The negative solutions (C_{12}, C_{13}, $C_{23} < 0$) have been rejected as unphysical because they did not satisfy the fundamental principle of lattice stability. In particular, all main minors of the elastic constant matrix were positive, as is required (Sirotin and Shaskolskaya 1979), only in the case when $C_{12} > 0$, $C_{13} > 0$ and $C_{23} > 0$.

The elastic compliances S_{ij} and linear elastic compressibility constants K_{ij} were determined at each temperature from the elastic constant matrix C_{ij}, using the following relations (Sirotin and Shaskolskaya 1979):

$$\begin{aligned}
&S_{11} = (C_{22}C_{33} - C_{23}^2)/A, && S_{22} = (C_{11}C_{33} - C_{13}^2)/A\,,\\
&S_{33} = (C_{22}C_{11} - C_{12}^2)/A, && S_{12} = (C_{13}C_{23} - C_{12}C_{33})/A\,,\\
&S_{23} = (C_{12}C_{13} - C_{11}C_{23})/A, && S_{13} = (C_{12}C_{23} - C_{22}C_{13})/A\,,\\
&S_{44} = 1/C_{44}, \quad S_{55} = 1/C_{55}, && S_{66} = 1/C_{66}\,,
\end{aligned} \tag{3}$$

where

$$A = \begin{vmatrix} C_{11} & C_{12} & C_{13} \\ C_{12} & C_{22} & C_{23} \\ C_{13} & C_{23} & C_{33} \end{vmatrix}, \qquad \begin{aligned} K_{11} &= S_{11} + S_{12} + S_{13}\,,\\ K_{22} &= S_{22} + S_{12} + S_{23}\,,\\ K_{33} &= S_{33} + S_{13} + S_{23}\,,\\ K_{12} &= 0, \quad K_{13} = 0, \quad K_{23} = 0\,. \end{aligned} \tag{4}$$

The temperature dependences of the elastic compliances $S_{ij}(T)$ and compressibility constants $K_{ij}(T)$ obtained in this way are presented in Figs 3 and 4 respectively. In spite of all expectations the anomalous changes in the elastic constants ΔC_{ij}, as well as in the elastic compliances ΔS_{ij} and compressibility constants ΔK_{ij}, are always continuous in the region of T_{I}. It should be noted that continuous changes of the elastic constants near T_{I} are observed also at relatively small rates of temperature change ($\sim 0{\cdot}05$ K min^{-1}). This unusual fact will be discussed below.

Using the experimental values of the C_{ij} matrix (Fig. 2), the wave velocity for any propagation direction can be calculated via equation (1). Figs 5 (Cs_2HgBr_4) and 6 (Cs_2CdBr_4) are polar plots of velocity versus propagation direction ($T = 293$ K) for propagation vectors in the XY, XZ and YZ planes respectively.

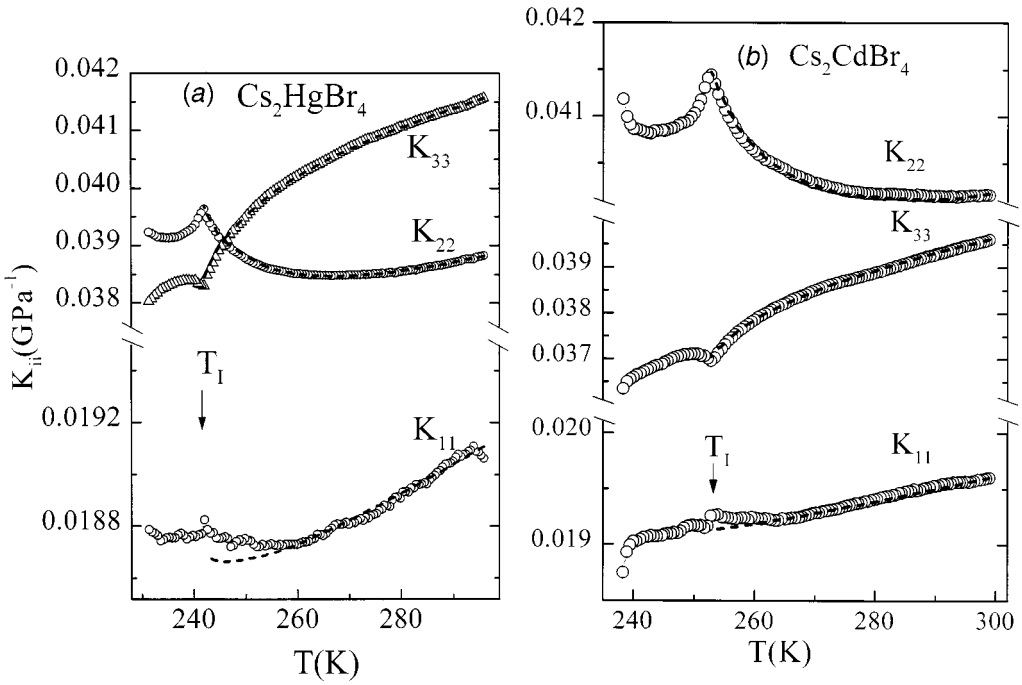

Fig. 4. Temperature dependences of the linear compressibility constants K_{ij} of (a) Cs_2HgBr_4 and (b) Cs_2CdBr_4 crystals.

It is immediately obvious that the velocities for transverse, quasitransverse and quasilongitudinal waves are nearly isotropic in the YZ plane for both compounds, whereas in the XY and XZ planes acoustical anisotropy is clearly observed, especially for the quasilongitudinal modes.

For each direction of propagation there are three associated wave modes, each with a different velocity, polarisation and ray energy propagation direction. The direction of energy flow in a crystal is, in general, not parallel to the propagation vector. The component of the ray direction, $\boldsymbol{R}(r_1,\ r_2,\ r_3)$, can be easily obtained using the following equations (Prawer *et al.* 1985):

$$\begin{aligned} r_1 &= lQ_jS_j + mQ_{6j}S_j + nQ_{5j}S_j\,, \\ r_2 &= lQ_{6j}S_j + mQ_{2j}S_j + nQ_{4j}S_j\,, \\ r_3 &= lQ_{5j}S_j + mQ_{4j}S_j + nQ_3jS_j\,, \end{aligned} \qquad \boldsymbol{S} = \begin{vmatrix} A_1^2 \\ A_2^2 \\ A_3^2 \\ 2A_2A_3 \\ 2A_3A_1 \\ 2A_1A_2 \end{vmatrix}\,, \tag{5}$$

where $\boldsymbol{A}(A_1, A_2, A_3)$ is the eigenvector of the matrix λ_{ij} (see equation 1). Figs 7 (Cs_2HgBr_4) and 8 (Cs_2CdBr_4) show plots of the magnitude of the angle between the ray direction and propagation direction, calculated via equation (5).

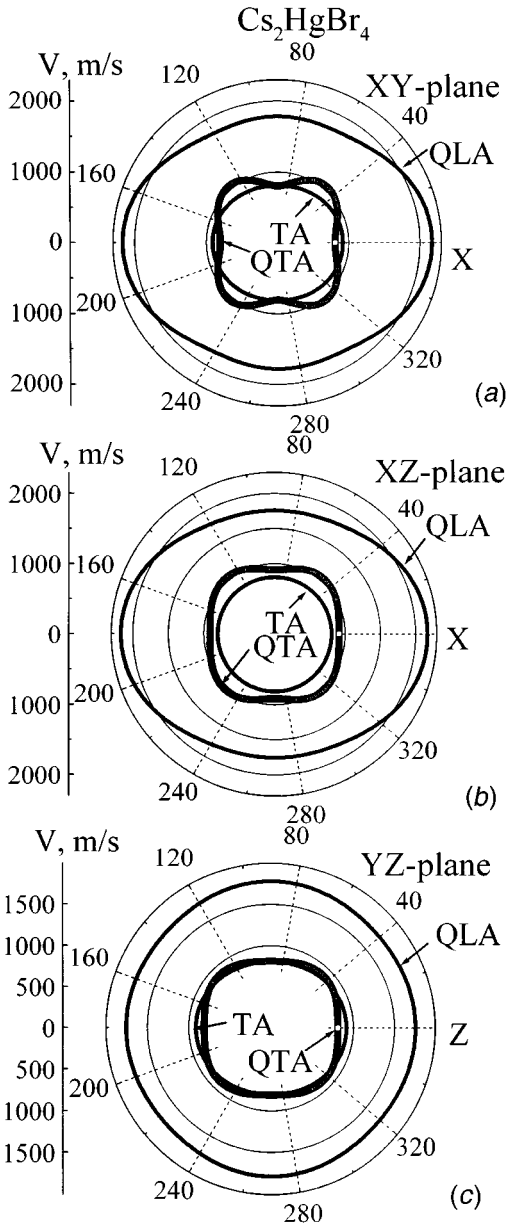

Fig. 5. Polar plots of the calculated phase velocity for the (*a*) *XY*, (*b*) *XZ* and (*c*) *YZ* planes of Cs_2HgBr_4 crystals.

A maximal deviation angle θ_M of about 40° is observed only in the *YZ*-plane for quasilongitudinal and quasitransverse waves of Cs_2HgBr_4. In all other cases the amplitude of θ_M is at most 25° for quasilongitudinal and quasitransverse modes, whereas for all pure transverse modes the deviation angle does not exceed even 10°. It is also obvious that the deviation angle $\theta = 0$ when α, β or $\gamma = 90n$ ($n = 0$, 1, 2, $\cdots$), which is demanded by symmetry. It is known that the deviation

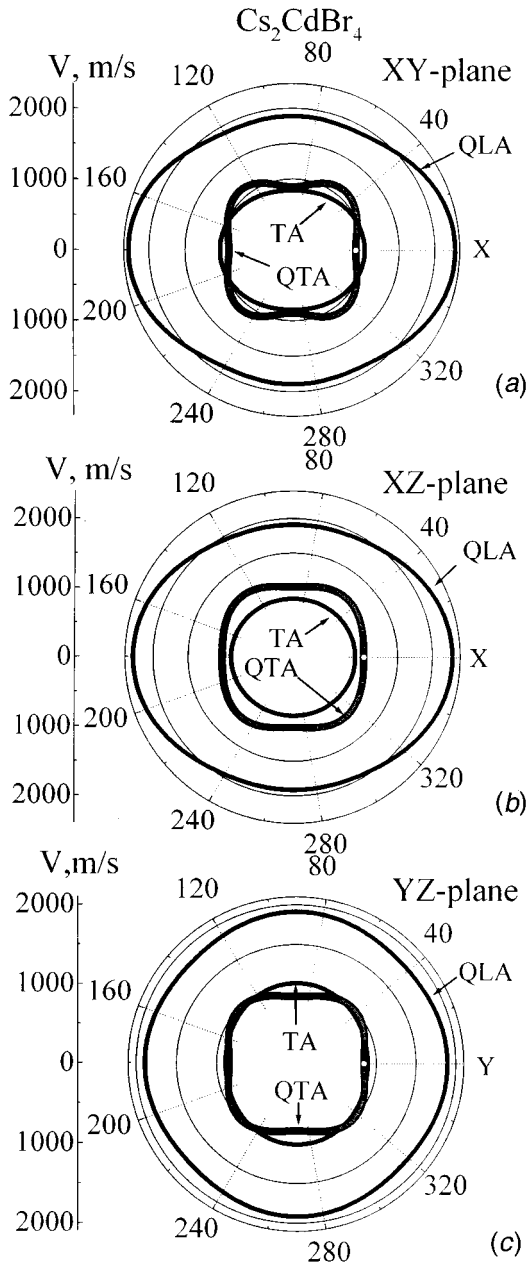

Fig. 6. Polar plots of the calculated phase velocity for the (*a*) *XY*, (*b*) *XZ* and (*c*) *YZ* planes of Cs_2CdBr_4 crystals.

angle θ, which defines the aperture and size of acousto-optical cells for a chosen geometry, is one of the most important parameters in acousto-optics. Usually it is desirable to have θ as small as possible, so Cs_2HgBr_4 and Cs_2CdBr_4 are rather suitable materials from this point of view. From another point of view, low values of ultrasonic velocities for both longitudinal and transverse modes enable us to

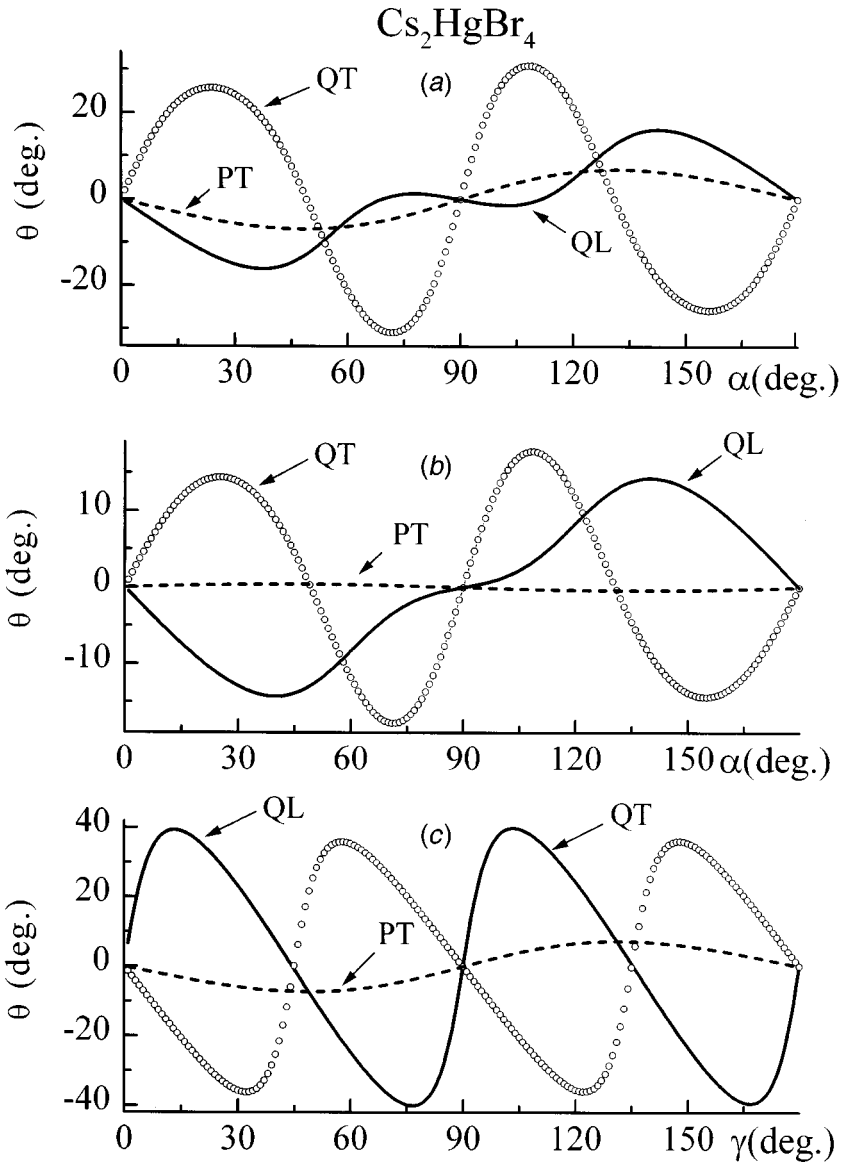

Fig. 7. Angle dependence of the deviation angle θ between the ray and propagation vectors for the (*a*) *XY*, (*b*) *XZ* and (*c*) *YZ* planes of Cs_2HgBr_4 crystals.

predict high acousto-optical parameters (diffraction angle Θ and acousto-optical quality M_2) in these crystals. Since $\Theta \sim V^{-1}$ and $M_2 \sim V^{-3}$ (Balakshyi *et al.* 1985), both these parameters are expected to have relatively high magnitudes. Moreover, Cs_2HgBr_4 and Cs_2CdBr_4 are optically biaxial crystals. Therefore they can be considered as relatively important materials for use in the construction of acousto-optical cells with low optical losses, which may be achieved using sample geometries with a wide range of acousto-optical interaction angles (Balakshyi *et al.* 1985). We note that the list of similar materials with good acousto-optical

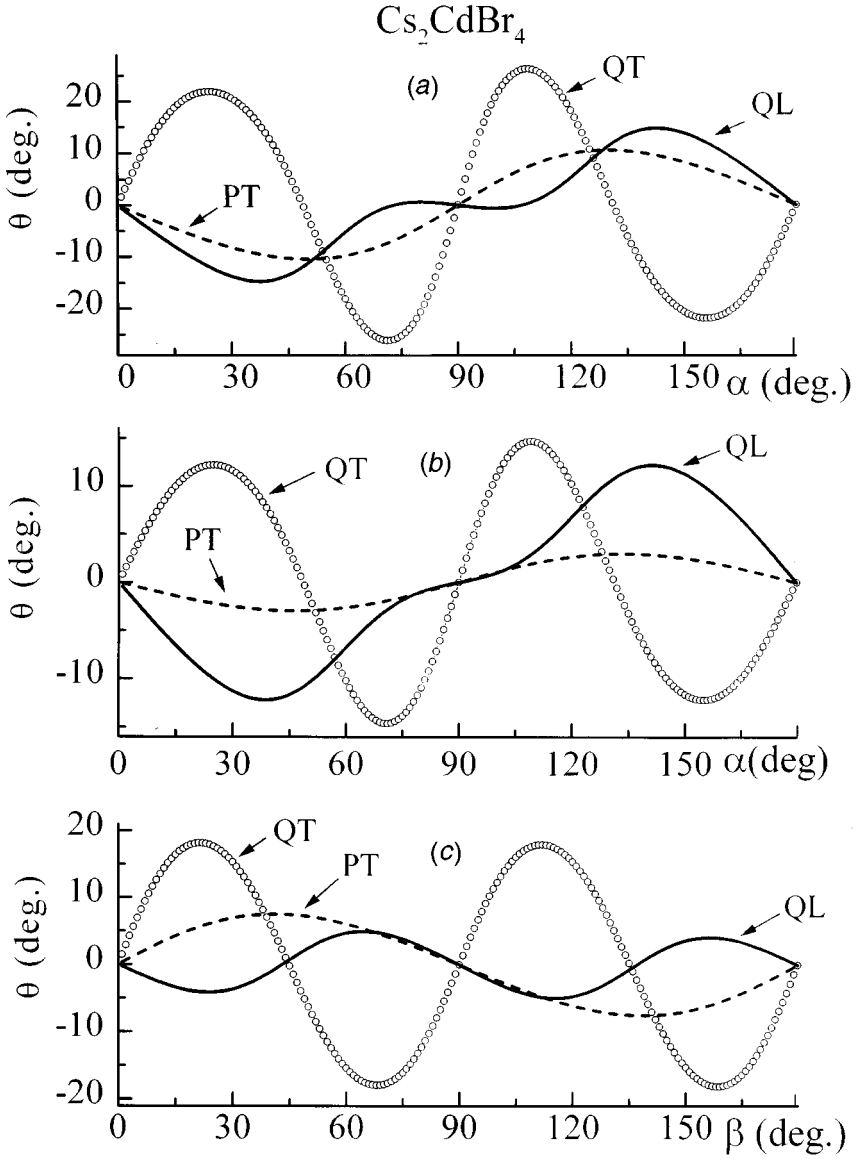

Fig. 8. Angle dependence of the deviation angle θ between the ray and propagation vectors for the (a) XY, (b) XZ and (c) YZ planes of Cs_2CdBr_4 crystals.

properties is not very long. Determination of the acousto-optical parameters of these materials will be reported in our subsequent papers.

Let us consider now the results obtained in the framework of the phenomenological theory. The elastic compliances S_{ij}, as well as the compressibility constants K_{ij}, are expressed through the elastic constants C_{ij} by equations (3) and (4). Therefore it is sufficient to consider the anomalous behaviour of separate elastic constants C_{ij}. The anomalous behaviour of the elastic constants in the region of the phase transition from the normal to the incommensurate phase is commonly explained

on the basis of a free-energy expansion with coupling terms that correspond to the anharmonic interaction between the strains U_1–U_6 and the order parameter. It is convenient to use as an order parameter the normal phonon coordinate Q_k which, according to symmetry considerations, belongs to the irreducible representation Σ_3 of the space-group symmetry of the high-temperature normal phase. The elastic part of the free energy in this case may be presented in the following form (Kityk *et al.* 1993):

$$F_{Q,U} = \tfrac{1}{2}\omega_k^2 Q_k Q_{-k} + \tfrac{1}{4}B(Q_k Q_{-k})^2 + \sum_{i=1}^{3} a_i O_k Q_{-k} U_i + \tfrac{1}{2}\sum_{i=1}^{6} b_{ii} Q_k Q_{-k} U_i^2 + \tfrac{1}{2}\sum_{\substack{i,j=1 \\ i\neq j}}^{3} b_{ij} Q_k Q_{-k} U_i U_j \,, \tag{6}$$

where $\omega_k^2 = A_0(T-T_\mathrm{I})+h(k_0-k)^2$ is the square of the soft-mode frequency, k is a wavevector, and a_i and b_{ij} are coupling constants that correspond to third- and fourth-order phonon–phonon anharmonic interactions respectively. Using equation (6) and taking into account the amplitudon–phason splitting below T_I (Dvorak and Petzelt 1978), we obtain the full elastic anomalies in the static limit ($\Omega\tau \ll 1$):

$$\Delta C_{ij} = -\frac{4a_i a_j |Q_{k0}|^2}{\omega_A^2(q)} + b_{ij}|Q_{k0}|^2 2 = 2a_i a_j/B + b_{ij}|Q_{k0}|^2, \quad i,j = 1\text{–}3\,, \tag{7a}$$

$$\Delta C_{ii} = b_{ii}|Q_{k0}|^2, \quad i = 4\text{–}6\,, \tag{7b}$$

where $\omega_A^2(q) = 2A(T_\mathrm{I}–T)+hq^2$ is the amplitudon frequency, and $|Q_{k0}|^2 = A_0(T_\mathrm{I}–T)/B$ is the equilibrium value of the order parameter amplitude. Only the behaviour of the shear elastic constants C_{44}, C_{55} and C_{66} is in good agreement with predictions of the phenomenological theory. The corresponding kinks or their temperature dependences (Fig. 2) at $T = T_\mathrm{I}$ are caused by the contribution of the order parameter amplitude (see equation 7b).

Following equation (7a), the value of the elastic constants C_{ij} (i,$j = 1$–3) would exhibit jump-like changes ($\Delta C_{ij} = –2a_i a_j/B$) at $T = T_\mathrm{I}$. The same anomalous behaviour is also predicted for the elastic compliances S_{ij} (i,$j = 1$–3) and compressibility constants K_{ij}. On the other hand, equation (7a) does not lead to any effect above T_I, contrary to the experimental evidence indicating pretransitional softening of the elastic constants in the normal phase. As usual, the origin of such behaviour is attributed to fluctuations. Following Levanyuk *et al.* (1992), the additional fluctuation contribution above T_I (in the static limit $\Omega\tau \ll 1$) may be presented as (see Kuzel *et al.* 1994):

$$\Delta C_{ij}^{\mathrm{fl}} = -a_i a_j F(T); \qquad F(T) = \frac{k_\mathrm{B} T_\mathrm{I}}{16\pi |C_x|^{3/2} [A_0(T-T_I)]^{1/2}}\,. \tag{8}$$

According to this formula C_{ij} should decrease when approaching T_I as is observed (see Fig. 2). However, the absence of jumps of C_{ij} (i,j = 1–3) at T_I

does not follow from the theory (Levanyuk *et al.* 1992). On the other hand, this theory does not take into account critical fluctuations, which appear very near T_{I}. According to Kuzel *et al.* (1994) these critical fluctuations can be responsible for the continuous changes of the static elastic constant C_{ij} in the vicinity of a normal–incommensurate phase transition. Using the dependence $F(T)$ determined from $C_{22}(T)$ (see Fig. 2) we have fitted the dependences of all the other elastic constants including the compliances S_{ij} $(i,j = 1\text{–}3)$ and compressibility constants K_{ij} in the normal phase. The dashed lines in Figs 2–4 are the best fits according to equation (8). The ratio between coupling constants, $a_1 : a_2 : a_3$, which defines the anisotropy of the fluctuation contribution, was found to be $0{\cdot}4 : 1 : 0{\cdot}4$ (Cs_2HgBr_4) and $0{\cdot}3 : 1 : 0{\cdot}27$ (Cs_2CdBr_4).

4. Conclusion

Using ultrasonic velocity measurements, all components of the elastic constant matrix C_{ij}, elastic compliances S_{ij}, and linear compressibility constants K_{ij} of orthorhombic Cs_2HgBr_4 and Cs_2CdBr_4 crystals have been determined in a wide temperature range including the region of the phase transition from the normal to the incommensurate phase. The elastic properties indicate clear anomalous temperature behaviour in the vicinity of the incommensurate phase transition. An explanation of the elastic anomalies near this transition is given in the framework of the phenomenological theory. Clear pretransitional softening of C_{ij}, S_{ij} and K_{ij} $(i,j = 1\text{–}3)$, observed in the normal phase, is attributed to fluctuations.

Cs_2HgBr_4 and Cs_2CdBr_4 crystals show relatively low values of the deviation angle between the ray direction and the propagation direction, as well as low values of the ultrasonic velocities of the longitudinal and transverse modes, which clearly indicates that both compounds should be rather effective materials in acousto-optical applications.

References

Balakshyi, B. I., Parygin, V. N., and Chirkov, L. E. (1985). 'Fizicheskije Osnovy Akusto-Optiki' (Radio i svjaz.: Moscow).

Bruce, A. D., and Cowley, R. A. (1978). *J. Phys.* C **11**, 3609.

Dvorak, V., and Petzelt, J. (1978). *J. Phys.* C **11**, 4827.

Kityk, A. V., Mokry, O. M., Soprunyuk, V. P., and Vlokh, O. G. (1993). *J. Phys. Cond. Matt.* **5**, 5189.

Kityk, A. V., Shchur, Ya. I., Zadorozhna, A. V., Trach, I. B., Girnyk, Y. S., Martynyuk-Lototska, I. Yu., and Vlokh, O. G. (1998). *Phys. Rev.* B (in press).

Kuzel, P., Dvorak, V., and Moch, P. (1994). *Phys. Rev.* B **49**, 6563.

Levanyuk, A. P., Minyukov, S. A., and Vallade, M. (1992). *J. Phys. (Paris)* **2**, 1949.

Maeda, M., Honda, A., and Yamada, N. (1983). *J. Phys. Soc. Japan* **52**, 3219.

Nakatama, H., Nakatama, N., and Chihara, H. (1987). *J. Phys. Soc. Japan* **56**, 2927.

Papadakis, E. P. (1967). *J. Acoust. Soc. Am.* **42**, 1045.

Plesko, S., Dvorak, V., Kind, R., and Treindl, H. (1981). *Ferroelectrics* **36**, 331.

Plesko, S., Kind, R., and Arend, H. (1980*a*). *Phys. Stat. Sol.* A **61**, 87.

Plesko, S., Kind R., and Arend, H. (1980*b*). *Ferroelectrics* **26**, 703.

Prawer, S., Smith, T. F., and Finlayson, T. R. (1985). *Aust. J. Phys.* **38**, 63.

Sirotin, Yu. I., and Shaskolskaya, M. P. (1979). 'Osnovy Kristallofiziki' (Nauka: Moscow).

Vlokh, O. G., Kaminskaya, E. P., Kityk, A. V., Levanyuk, A. P., and Mokry, O. M. (1989). *Sov. Phys. Solid State* **31**, 1629.

Manuscript received 30 April, accepted 1 September 1998